REPORT DOCUMENTATION PAGE

Form Approved
OMB No. 0704-0188

Public reporting burden for this collection of information is estimated to average 1 hour per response, including the time for reviewing instructions, searching existing data sources, gathering and maintaining the data needed, and completing and reviewing this collection of information. Send comments regarding this burden estimate or any other aspect of this collection of information, including suggestions for reducing this burden to Department of Defense, Washington Headquarters Services, Directorate for Information Operations and Reports (0704-0188), 1215 Jefferson Davis Highway, Suite 1204, Arlington, VA 22202-4302. Respondents should be aware that notwithstanding any other provision of law, no person shall be subject to any penalty for failing to comply with a collection of information if it does not display a currently valid OMB control number. **PLEASE DO NOT RETURN YOUR FORM TO THE ABOVE ADDRESS.**

1. REPORT DATE *(DD-MM-YYYY)*
30-06-2003

2. REPORT TYPE
Technical Paper

3. DATES COVERED *(From - To)*

4. TITLE AND SUBTITLE

Study of Energy Loss Mechanisms in the BPT-4000 Hall Thruster

5a. CONTRACT NUMBER

5b. GRANT NUMBER

5c. PROGRAM ELEMENT NUMBER

6. AUTHOR(S)

Kristi de Grys, Chris Rayburn (Aerojet); James Haas (AFRL/PRSS)

5d. PROJECT NUMBER
1011

5e. TASK NUMBER
0009

5f. WORK UNIT NUMBER

7. PERFORMING ORGANIZATION NAME(S) AND ADDRESS(ES)

Air Force Research Laboratory (AFMC)
AFRL/PRSS
1 Ara Drive
Edwards AFB CA 93524-7013

8. PERFORMING ORGANIZATION REPORT NUMBER

AFRL-PR-ED-TP-2003-179

9. SPONSORING / MONITORING AGENCY NAME(S) AND ADDRESS(ES)

Air Force Research Laboratory (AFMC)
AFRL/PRS
5 Pollux Drive
Edwards AFB CA 93524-7048

10. SPONSOR/MONITOR'S ACRONYM(S)

11. SPONSOR/MONITOR'S NUMBER(S)
AFRL-PR-ED-TP-2003-179

12. DISTRIBUTION / AVAILABILITY STATEMENT

Approved for public release; distribution unlimited.

13. SUPPLEMENTARY NOTES

For presentation at the AIAA Joint Propulsion Conference in Huntsville, AL, taking place 20-23 July 2003.

14. ABSTRACT

20030812 210

15. SUBJECT TERMS

16. SECURITY CLASSIFICATION OF:			17. LIMITATION OF ABSTRACT	18. NUMBER OF PAGES	19a. NAME OF RESPONSIBLE PERSON
					Leilani Richardson
a. REPORT	b. ABSTRACT	c. THIS PAGE	A	10	19b. TELEPHONE NUMBER *(include area code)*
Unclassified	Unclassified	Unclassified			(661) 275-5015

Standard Form 298 (Rev. 8-98)
Prescribed by ANSI Std. 239.18

Joint Propulsion Conference
Huntsville, AL July 20-23, 2003

STUDY OF POWER LOSS MECHANISMS IN THE BPT-4000 HALL THRUSTER*

Kristi de Grys* and Christopher Rayburn+
Aerojet
Redmond, WA

James Haas
Air Force Research Laboratory
Edwards Air Force Base, CA

ABSTRACT

Aerojet has developed a high performance multi-mode flightweight Hall thruster for orbit raising and stationkeeping on geo-synchronous satellites. In order to further understand and improve upon the performance of this state of the art Hall thruster and other next generation thrusters being planned, a detailed study of the energy loss mechanisms has been conducted. Calculations of each loss mechanism have been performed using experimental data as input. A comparison of the relative magnitude of each loss mechanism shows that energy deposition in the anode and radial kinetic energy are the dominant losses in this thruster followed by energy deposition in the insulator rings. The calculations also show that the propellant utilization efficiency is only 70% but the voltage losses are minimal. These results indicate potential for improved performance of this and other next generation thrusters if the electron-neutral collision frequency can be increased and the ion beam acceleration focused with improved magnetic field and anode designs.

NOMENCLATURE

d	Distance between thruster exit plane and measurement location, m
E_i	Ionization energy, eV
f_z	Species fraction at 1 m, %
F_i	Ion flux, A/cm^2
I_{beam}	Total ion beam current at the exit plane, A
I_{dis}	Discharge current, A
I_{meas}	Total measured ion beam current at 1 m, A
k	Boltzmann constant, J/K
l	Path length, m
m_{an}	Anode mass flow rate, mg/s
m_{cat}	Cathode mass flow rate, mg/s
m_e	Electron mass, kg
m_{Xe}	Xenon atom mass, kg
n_n	Neutral density, m^{-3}
N_A	Avogadro's number, mol^{-1}
N_e	Electron number per unit time, s^{-1}
N_i	Ion number per unit time, s^{-1}
P_{dir}	Directed power, W
P_{ioniz}	Power consumed in ionizing propellant, W
q	Charge magnitude, C
T	Thrust, mN
T_e	Electron temperature, eV
T_i	Ion temperature, K
T_{nan}	Neutral temperature at anode, K
T_{ncat}	Neutral temperature at cathode, K
v_z	Ion velocity, m/s
V_{dis}	Applied discharge voltage, V
V_i	Energy per unit charge, V
w_{mol}	Molecular weight of xenon, kg/mol
ϕ	Angle from thruster centerline, rad
η	Thrust efficiency, %
η_a	Ratio of beam current to discharge current, %
η_e	Ion acceleration efficiency, %
η_u	Propellant utilization efficiency, %
σ_z	Collision cross section, m^2

INTRODUCTION

As shown by numerous mission studies, Hall thrusters offer significant advantages for earth orbit applications over other EP devices because they provide a combination of high thrust to power and

* Development Engineer, Member AIAA
+ Development Engineer, Member AIAA

Approved for public release; distribution unlimited.

high I_{sp}.[1,2] As such, significant investments have been made by the Air Force, NASA and industry towards the development of Hall thrusters. These investments have lead to the rapid maturation of the technology in the United States and the current baselining of the BPT-4000 multi-mode Hall thruster for orbit topping and station keeping on the AEHF satellites.[4] While a variety of electric propulsion devices including arcjets, ion thrusters, and Russian Hall thrusters have been widely accepted for station keeping applications, the AEHF satellites will mark the first use of a medium power Hall thruster for orbit raising on military or commercial satellites.

Despite the continuing maturation of Hall thruster technology, there are a wide variety of missions that could benefit from or would be enabled by next-generation Hall thruster technology such as orbit transfer vehicles and nuclear powered spacecraft. These new applications, however, require expanding the operating bounds of these devices beyond those of current flight models. Future missions require higher thrust to power, higher I_{sp}, and higher power operation as well as extended life capability. Achieving these gains requires a detailed understanding of the variables that control the performance of these devices.

To add to that understanding as well as provide a potential near term benefit to the AEHF program, Aerojet and AFRL have been looking in detail at the performance characteristics of the BPT-4000 Hall thruster. The primary goal of the program is to understand and eliminate the performance decrease seen over the first 200 hours of operation of this thruster and other Hall thrusters such as the SPT-100.[5] Additional benefits will also likely be gained through the development of a deeper understanding of the design features that control the performance of these thrusters.

As part of this effort, Aerojet performed an energy balance study of the BPT-4000 Hall thruster to quantify the power loss mechanisms. The objective of the study was to identify the dominant loss mechanisms in order to gain insight into design changes that could be made to reduce these losses. This paper presents the methodology used to calculate the fractional power losses and the quantitative results.

BACKGROUND

METHODOLOGY

The basic methodology used in the study was to draw a control volume around the thruster and appropriately account for all energy input and output. The downstream extent of the control volume was defined as the point where ion acceleration has reached its maximum extent. Based on near field ion velocity measurements made on other thrusters that this location is typically on the order of 5 cm beyond the exit plane as defined by the downstream surface of the magnet poles.[6,7] The other boundaries of the control volume were chosen to be the physical boundaries of the thruster - the mounting surface and the outer diameter.

The input power to the control volume was assumed to be in the form of voltage and current delivered from laboratory power supplies or a power processing unit (PPU). The numerous forms of power loss are illustrated in Figure 1 and calculation of the dominant mechanisms is discussed in the following sections.

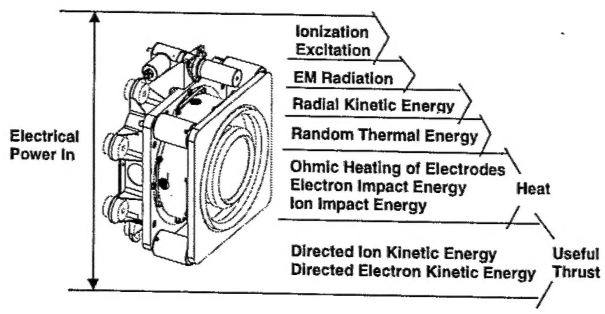

Figure 1 - BPT-4000 Hall Thruster Power Balance

The analysis drew heavily from the existing database of experimental data available on BPT-4000 laboratory and engineering development model Hall thrusters. These data were taken both by Aerojet and by other independent government entities and universities and is generally in the public domain and referenced as applicable.

ION PLUME

The bulk of the electrical power is converted into kinetic energy that leaves the thruster in the ion plume. The energy the ions carry with them can be divided into radial and directed kinetic energy, random thermal energy and excitation energy.

Kinetic Energy

The kinetic power exiting the thruster has both a directed component producing thrust and a radial component which is a loss mechanism subsequently referred to as radial losses. Assuming

measurements of current flux versus energy to charge data as a function of angle are available, the radial and directed power can be calculated from the following equations:

$$P_{dir} = \sum_{\phi=0}^{\pi/2} \sum_{V=0}^{V_{max}} \frac{df}{dV_i}(V_i, \phi) * \Delta V_i * \left(2\pi d^2 \sin(\phi)\cos(\phi)\Delta\phi\right) * V_i$$

$$P_{rad} = \sum_{\phi=0}^{\pi/2} \sum_{V=0}^{V_{max}} \frac{df}{dV_i}(V_i, \phi) * \Delta V_i * \left(2\pi d^2 \sin^2(\phi)\Delta\phi\right) * V_i$$

where d is the distance between the thruster exit plane and the measurement location, ϕ is the angle from the thruster centerline, and V_i is the energy per charge (E/q).

While detailed plume measurements have been made on a BPT-4000 laboratory thruster, the measured performance of this thruster and its design are described elsewhere.[8,9] The issue with Pollard's measurements for the purposes of this calculation is that they were made at 1 m from the thruster exit plane and no data is available for angles between 0 and 20 degrees from centerline.

To compensate for the lack of data between 0 and 20 degrees, it was assumed that the relative distribution of the ion energies remained constant from centerline to 20 degrees. The ion current for each angle was then adjusted based on the ratio of the measured ion current at the angle in question to that measured at 20 degrees from Faraday cup measurements also made at 1 m.

The validity of this assumption was assessed in several ways. King and Gallimore's data on the SPT-100 from 1 m shows excellent agreement between the energy distribution at 20 degrees and along the centerline.[10] The agreement is much poorer at 10 degrees where the magnitude of the first higher peak on the energy spectrum is on the same order as the primary peak. The same behavior is not seen in unpublished measurements made on another version of the BPT-4000 laboratory thruster using the same setup. In these measurements, the ion energy distribution remains nearly identical between 0 and 20 degrees. Pollard and Beiting also made measurements on the SPT-140 using the same apparatus as was used on the BPT-4000.[6] At 2.0 kW, 300 V, they were able to make measurements to 10 degrees. The results support the conclusion that the overall energy distribution is relatively constant between 10 and 20 degrees.

The total current under the df/dV distribution was also integrated overall energies and angles. The total current was found to be 5.52 A which agreed within 2% with the 5.4 A of total current from Faraday cup measurements made by Pollard for the same operating condition.[8] Therefore, the authors believe that the assumption that ion energies remained constant from centerline to 20 degrees is sufficient for the purposes of this analysis.

The second effect that must be accounted for is that the plume data were taken at 1 m, whereas the exit of the calculation box was defined to be 5 cm downstream of the thruster exit plane. Between 5 cm and 1 m the ion plume interacts with itself and with the background neutral gas. The most significant of these interactions is ion-neutral charge exchange where ions collide with a neutral gas atom and transfer one or more electrons. The net effect of these collisions is a reduction in the measured ion current at 1 m. The true current at the exit plane, I_{beam} is given by the following equation:

$$I_{beam} = \sum_{Z=0}^{3} f_Z I_m \frac{1}{1 - n_n \ell \sigma_i}$$

where σ_i is the effective collision cross section for each species, n_n is the neutral density, l is the path length, I_m is the measured current at the path length, and f_Z is the measured species fraction as a function of charge state at 1 m. The collision cross sections for $Xe^+ + Xe \rightarrow Xe + Xe^+$, $Xe^{2+} + Xe \rightarrow Xe + Xe^{2+}$, and $Xe^{2+} + Xe \rightarrow 2Xe^+$ have been measured over the energy range of interest by Pullins et al.[11] For singly ionized xenon from 1 to 300 eV, the cross section in A^2 as a function of ion energy can be approximated by the following equation:

$$\sigma_{Xe^+ \rightarrow Xe}\left(v_{Xe^+}\right) = (188.81 - 23.30\log(v_{Xe+}))\left(\frac{12.13}{13.6}\right)^{-1.5}$$

where v_{Xe+} is the xenon ion velocity and the coefficients are given by a fit of the experimental data. Pullins et al performed no measurements above 300 eV. For the purposes of this analysis, it was assumed that the relationship was the same at higher energies.

For doubly ionized xenon resonant charge exchange, $Xe^{2+} + Xe \rightarrow Xe + Xe^{2+}$, the cross section as a function of ion energy can be approximated by a second equation of the same form:

$$\sigma_{Xe^{2+} \rightarrow Xe}\left(v_{Xe^{2+}}\right) = (94.4 - 11.65\log(v_{Xe++}))\left(\frac{12.13}{13.6}\right)^{-1.5}$$

In this case, data were taken up to 600 eV energies. The authors are unaware of any cross sectional data available in the literature for Xe^{3+} charge exchange probabilities. Therefore, the cross section for $Xe^{3+} + Xe \rightarrow Xe + Xe^{3+}$ was taken to be 33% of the cross section for $Xe^{+} + Xe \rightarrow Xe + Xe^{+}$. The basis for this selection was the ratio of the cross sections of Xe^{+} and Xe^{2+}.

For the majority of the distance between the exit plane and 1 m, the neutral density is dominated by the background chamber gas. By contrast, the neutral density in the near field is approximately an order of magnitude higher due to neutralizer flow and primary thruster flow which passes through the discharge channel without being ionized.[12] Since the fractional reduction in beam current due to charge exchange is linear in neutral density and distance, an average density of 8.8×10^{17} m^{-3} was calculated for the 1 m distance using Katz's calculations and using a neutral background pressure of 9.6×10^{-5} Torr as measured by Pollard.[8]

No corrections were performed for non-resonant ion-neutral charge exchange collisions such as $Xe^{+2} + Xe \rightarrow 2Xe^{+}$. The high energy ion produced from this collision assuming no momentum exchange shows up as a peak in E/q spectrum at twice the value of the primary peak as has been discussed by others.[6,10] Because the resultant ions produce a signature with twice the original current at half the original voltage, the power is unchanged and no correction is required. The same argument holds for non-resonant charge exchange interactions of Xe^{3+} ions.

Although the power is unchanged, the species fractions at 1 m are altered by non-resonant charge exchange collisions. Pullins et al. found that for Xe^{2+} the non-resonant charge exchange cross section is an order of magnitude lower than that for resonant charge exchange. Data are available between 0 and 600 eV. Below 300 eV, the cross-section is negligible. For 568 eV Xe^{2+} ions, the fractional reduction in current for the neutral density discussed above is ~12%. Therefore, only approximately 1% of the Xe^{2+} beam ions undergo non-resonant charge exchange. This estimate is consistent with the peak at 568 V which is two orders of magnitude less than the peak. Because the percentage of double and triple ions is ~10% the 1% of these that undergo non-resonant charge exchange represents less than 0.1% of the total ions. Therefore, the effect of non-resonant charge exchange collisions on the species fractions is neglected.

In addition to charge exchange collisions, beam ions also undergo elastic scattering collisions between the exit plane and the measurement location at 1 m. The dominant elastic scattering is between charged ions from the primary peak and background gas neutrals. This ion-neutral elastic scattering is discussed in detail by Katz et al. and results in a peak in the energy spectrum whose energy varies as a function of the angle from centerline.[12] These collisions involve only momentum transfer so they do not affect the overall species fractions or total current. However, they do cause the total power measured at 1 m to be less and they increase the number of ions measured at higher angles off centerline which increases the apparent radial losses. Since a detailed model which accounts for scattering was not available for back extrapolation, several simplifying assumptions were made. The full beam current was assumed to be ejected from the centerline, to consistent entirely of singly charged xenon, and to have an energy per ion of 284 eV. The total cross section and average scattering angle were calculated using the following equations:

$$\sigma_{tot} = 2\pi \int_0^{\pi/2} \frac{d\sigma}{d\Omega}(\theta)\sin(\theta)d\theta$$

$$\theta_{avg} = \frac{\int_0^{\pi/2} \frac{d\sigma}{d\Omega}(\theta)\sin(\theta)\theta d\theta}{\int_0^{\pi/2} \frac{d\sigma}{d\Omega}(\theta)\sin(\theta)d\theta}$$

The final total cross section was found to be 161 A^2 and the average angle 6.3° using cross section data from Katz et al.[12]

The correction for this effect was applied at the very top level to P_{dir} and P_{cos} by modifying the equations to the following:

$$P'_{dir} = P_{dir} + (1 - \sigma_{tot} n_n \ell) I_{tot} (1 - \cos^2 \theta_{avg}) V_{peak}$$
$$P'_{rad} = P_{rad} - (1 - \sigma_{tot} n_n \ell) I_{tot} (1 - \cos^2 \theta_{avg}) V_{peak}$$

The overall correction is ~1% since although most ions undergo an elastic collision, the average energy lost is small (< 5 eV).

Ion-ion elastic scattering collisions also occur. Since these collisions do not involve a neutral atom, there is no net effect on the total power measured since

for every ion that loses energy, another ion gains energy. These collisions also have no effect on the total species fraction since charge exchange is not involved. They do, however, alter the angular distribution which will slightly increase the apparent cosine losses. No corrections were made to account for this effect.

It is interesting to note that this analysis is inconsistent with near field species fraction measurements made at 10 cm by Gulczinski and Gallimore on the Michigan P5 thruster.[13] Their measurements showed the fraction of Xe^+ ions in the primary peak increased by 29% between 10 cm and 75 cm with a corresponding decrease in the fraction of Xe^{2+} ions. Given the cross sections measured by Pullins et al, one cannot explain the change by charge exchange since the cross section for Xe^{2+} charge exchange is less than that for Xe^+. Elastic scattering therefore seems the only possibility. The validity of this explanation could have been tested by making species fraction measurements in the near and far field at other energies and at other angles. Assuming elastic scattering caused the change, one would expect to see a substantial reduction in the fraction of Xe^{2+} ions measured at E/q ratios below 284 V from the far field to the near field. These measurements were not performed. However, this conclusion is supported by the significant fraction of Xe^{2+} ions measured at E/q ratios below 200 V in the far field at 0 degrees.

Species fraction measurements in the far field were made by Pollard et al on the BPT-4000 at several E/q ratios.[8] These measurements show very little change in the species fraction as a function of energy. This result is consistent with the previous analysis but inconsistent with Gulczinski and Gallimore's measurements. Therefore, it seems unlikely that the species fractions in the near field of the BPT-4000 are dramatically different than those in the near field. Without detailed knowledge of P5 thruster, it is postulated that the high rate of elastic scattering collisions observed with this thruster is related to operating it at a very low power density compared to nominal (1600 W versus 5000 W). Low power density operation of Hall thrusters is typically characterized by very inefficient operation and ejection of ions with higher radial velocity components.

Thermal Energy

The power leaving the thruster in the form of ion thermal energy is given by the following equation:

$$P_{itherm} = \frac{3}{2} N_i k T_i$$

where N_i is the number per unit time of ions leaving the thruster and T_i is the ion temperature in K. The temperature of the ions was assumed to be the same as the neutral gas prior to ionization. Since the neutral gas is injected into the discharge channel through the anode, the temperature of the ions is taken to be equal to the anode temperature or 925 K for 3 kW, 300 V operation. N_i was calculated from the following equation:

$$N_i = \sum_{\theta=0}^{\pi/2} \frac{I_o(\theta)\Delta\theta}{q_{avg}(\theta)}$$

where $I_o(\theta)$ is the total current enclosed in ring of width $\Delta\theta$ (5°) at an angle of θ from centerline and $q_{avg}(\theta)$ the averge charge both calculated from the spectrum 5 cm downstream of the thruster exit plane.

Excitation Energy

Ions (and neutrals) leaving the thruster have typically been excited by multiple collisions with electrons. This excitation energy is gradually lost through the emission of visible and ultraviolet light as the excited states decay to the lowest energy state. Careful measurements of the power in these radiated optical emissions were made on the SPT-100 by Manzella.[14] These measurements showed that < 0.02% of the total power was lost. Since the total power lost was such a small fraction, this power was neglected in the analysis.

IONIZATION LOSSES

The energy consumed in ionizing the propellant is given by the following equation:

$$P_{ioniz} = \sum_{\theta=0}^{\pi/2} \frac{I_{beam}(\theta)\Delta\theta}{q_{avg}(\theta)} \begin{bmatrix} E_{Xe+} + (\%Xe^{2+}(\theta) + \%Xe^{3+}(\theta))E_{Xe2+} \\ + \%Xe^{3+}(\theta) * E_{Xe3+} \end{bmatrix}$$

where $I_{beam}(\phi)$ is the total current enclosed in ring of width $d\phi$ (5°) at angle of ϕ from centerline, E_{Xei} are the respective ionization energies given in Table 1, and $\%Xe^i(\phi)$ is the fraction of each species at the exit plane. The species fractions at the exit plane were calculated based on the current spectrum corrected for charge exchange. The correction increased the fraction of Xe^+ from 80% to 83% with a corresponding decrease in the fraction of Xe^{2+} and Xe^{3+}.

Table 1: Xenon Ionization Potentials

Charge State	Ionization Potential
Xe^{+}	12 eV
Xe^{2+}	33 eV
Xe^{3+}	65 eV

ELECTRON AND NEUTRAL PLUMES

Electron Plume

As with the ion plume, the power the electrons carry with them can be divided into kinetic energy - useful thrust and radial losses and random thermal energy. The random thermal energy of the electrons is given by the following equation:

$$P_{etherm} = \frac{3}{2} N_e k T_e$$

where N_e is the number per unit time of electrons leaving the thruster and T_e is the ion temperature in eV. The electron temperature used was from measurements made by Pollard et al. at a distance of 0.5 m from the thruster exit plane for 3 kW, 300 V operation.[8] Since the electron temperature measurements varied by only 0.5 eV overall angles and showed no particular trend, a constant electron temperature of 2.2 eV was used. N_e was taken to be equivalent to N_i since the plasma is quasi-neutral.

The directed kinetic energy carried by the electrons is given by the following equation assuming quasi-neutrality in the plume:

$$P_{edir} = P_{dir} \frac{m_e}{m_{Xe}}$$

where m_e is the electron mass, m_i is the mass of a xenon atom, and P_{dir} is the directed power in the ion plume. Since $m_e/m_{Xe} << 1$, the directed power of the electrons can be neglected.

Neutral Plume

The power contained in the neutral plume is due to the thermal energy of the unionized xenon atoms leaving the thruster and cathode and is given by the following equation:

$$P_{neut} = \frac{3}{2}\left(\frac{\dot{m}_{an} N_A}{m_{Xe}} - N_i\right) k T_{nan} + \frac{3}{2}\left(\frac{\dot{m}_{cat} N_A}{m_{Xe}}\right) k T_{ncat}$$

where m_{an} is anode mass flow rate, m_{cat} is the cathode mass flow rate, T_{nan} is the neutral temperature in K of neutrals coming from the thruster, and T_{ncat} is the temperature of neutrals leaving the keeper orifice. The temperature of the neutrals leaving the thruster is assumed to be the same as the ion temperature and equal to the anode temperature since the gas in the BPT-4000 thruster design is injected through the anode. The temperature of the neutrals leaving the cathode is assumed to be equal to the keeper temperature. While these temperatures have not been verified experimentally, the amount of power carried away by the neutrals is less than 0.05% so the temperatures would have to be off by more than an order of magnitude to affect the results of the analysis.

THERMAL LOSSES

To obtain estimates for the cathode and thruster thermal losses, a combination of temperature measurements and finite element modeling were used.

For the thruster, temperature measurements were made on the laboratory thruster discussed in Reference 6. Energy is deposited in the thruster due to collisions of electrons, ions and neutrals with the insulator walls and the anode channel. This energy was measured by isolating the discharge channel with a single conductive path and placing thermocouples known distances apart as shown schematically in Figure 2 (not to scale).

The difference in temperature between each pair of thermocouples was used to calculate the conductive heat transfer and the measured surface temperatures were used to estimate the radiative losses. Post-measurement calculations showed the fraction of energy deposited in each of the insulator rings and the anode region. The key uncertainty in this approach is the emissivity of the materials since radiative losses dominate. Emissivities used were based on measurements performed by Lockheed Martin on the specific materials in question.

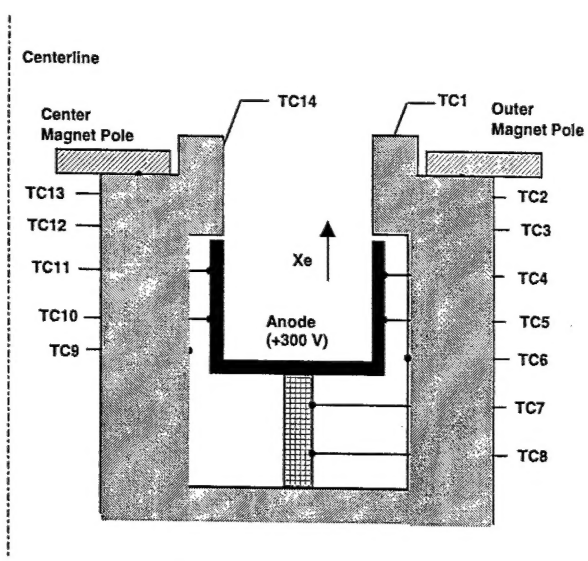

Figure 2 - Temperature Measurement Setup

The final calculated power deposition numbers were verified by correlating the temperatures predicted by a TMG finite element model of the engineering development thruster with temperature measurements. The calculated dissipation values were used as inputs and were distributed between the anode and the inner and outer insulator rings accordingly. A radiative environment that simulated the test cell was assumed and the mounting interface temperature was fixed at the measured temperature of the thruster mounting bracket during steady state operation.

The measured and predicted values for equilibrium operation at 3.0 and 4.5 kW showed excellent agreement. Due to the geometry of the EDM thruster, thermocouples could not be imbedded in the insulator rings but equilibrium temperature measurements were made on all other key components. The predictions were within ±6% of the measurements with the model overpredicting in some regions and underpredicting in others. The areas of discrepancy were likely due to the uncertainty in the conduction across bolted interfaces rather than errors in the input power.

Cathode thermal losses were estimated in a similar fashion. During steady state operation, the heat flux into the cathode is driven by the internal plasma. NASA and Aerojet cathode data show the heat flux is primarily a function of emission current and only a very weak function of the xenon mass flow rate through the cathode.[15,16] To estimate the heat flux, measurements of cathode orifice plate temperature as a function of current were correlated with the temperature as a function of heater power. The derived relationship gives the following equation relating discharge current to power dissipation:

$$P_{thermcat} = 0.6*(0.011 I_{dis}^{3} - 0.23 I_{dis}^{2} + 3.2 I_{dis} + 21)$$

Measurements of orifice plate temperature were made with a Leeds and Northrup single color optical pyrometer. The pyrometer had previously been correlated in the setup with thermocouple measurements made on another cathode with holes in the keeper to allow installation of thermocouples.

As with the thruster power dissipation measurements, the cathode power dissipation relationship was verified by comparing the temperatures predicted from a TMG finite element model of the EDM cathode with thermocouple measurements. In this case, the correlation was even better with all measured data with 4% of the predictions.

RESULTS

Table 2 shows a summary of the calculated power breakout and the total calculated power and efficiency.

Table 2 - Calculated Power Distribution

Component	Magnitude
Ion Directed Power	1793 W
Heat Loss	775 W
Ion Radial Loss	385 W
Primary Ionization	69 W
Multiple Ionization	63 W
Total Power	**3085 W**
Total Efficiency	**58%**

The calculated results show excellent agreement with measurements of input power and total efficiency. The total calculated output power is only 2.8% higher than the 3000 W input which well within the uncertainty of the calculations. The calculated efficiency of the thruster is 60% compared to a measured efficiency for this thruster of 58% again showing excellent agreement. The small discrepancy is likely due to an overestimate of the heat loss. If the heat loss were 85 W lower, the total calculated efficiency would agree exactly with the measured efficiency. One would also expect that the calculated efficiency would be slightly lower than the measured since ion-ion elastic collisions were not taken into account. The directed power calculation is also highly sensitive to the average neutral density used in the charge exchange calculations. Measurements of background chamber pressure are typically accurate to only +/- 20% so this uncertainty also contributes to the deviation from the measured efficiency. Given the uncertainties in all of the measurements, the fact that the calculations are within less than 3% is excellent.

Figure 3 shows the fractional breakout of the total power. The pie chart clearly shows that over half of the lost power goes into heat. The heat flux measurements show that over 60% of this heat goes directly into the anode. Assuming the flux of ions to the anode is negligible, the average energy of each electron hitting the anode is 43 eV. Electron temperature measurements have been made in the anode region on various other Hall thrusters and show temperatures ranging from 2 to 32 eV with

most regions in the 5 to 15 eV range which is also what is predicted by most models.[17,18]

Figure 3 - Distribution of Power in BPT-4000 Laboratory Model Hall Thruster

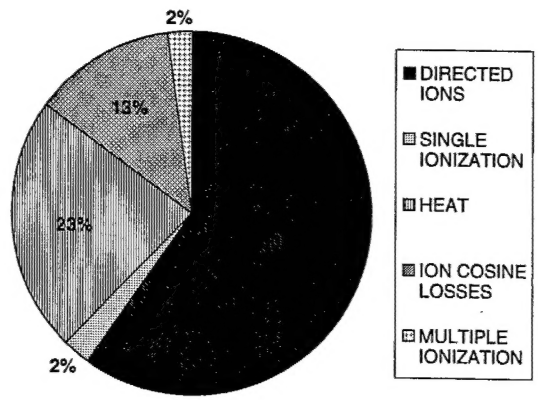

Therefore, the 43 eV energy would appear higher than one might have expected. There are several possible reasons for the difference. The first is the radically different anode configuration of the BPT family thrusters.[19] All of the referenced measurements were made on thrusters where the axial walls of the anode region are ceramic. In BPT type thrusters, the metal walls extended 10+ mm farther downstream towards the ionization zone. The electron energy is also influenced by the anode sheath which is not accounted for in the electron temperature measurements. Third, none of the measurements were made in the very near anode region and the measurements also indicate that the electron temperature may increase as the anode surface is approached. One or a combination of these likely accounts for the higher electron energies implied by the energy loss analysis.

A related measure of thruster performance is the propellant utilization efficiency. This quantity can be calculated from the following equation knowing the total ion beam current and the species fractions at the downstream end of the control volume:

$$\eta_u = \frac{\dot{m}_i}{\dot{m}} = \frac{I_{beam} m_{wXe}}{q_{avg} N_A \dot{m}}$$

where I_{beam} is the total ion beam current, q_{avg} is the average charge, m is the anode mass flow rate, N_A is Avogadro's number, and m_{wXe} is the molecular weight of xenon. Using the values for these quantities calculated above, one finds that the propellant utilization efficiency of the BPT-4000 Hall thruster is approximately 71% (not including neutralizer flow). The SPT-100 on the other hand which has overall lower performance has a reported propellant utilization efficiency of 95%.[20] The rather low value of the BPT-4000 utilization compared to other Hall thrusters coupled with the high energy of electrons reaching the anode suggests that significant gains in performance could be achieved by increasing the collision frequency of electrons and neutrals in the ionization region.

Given that the propellant utilization efficiency of the BPT-4000 Hall thruster is significantly lower than that of the SPT-100 but the performance is higher, it is interesting to compare the values of the three components that drive the efficiency of a Hall thruster. As presented by Fife and Martinez-Sanchez[20], the total efficiency of a Hall thruster is given by the following equation:

$$\eta = \eta_u \eta_a \eta_e$$

where η_u is the propellant utilization efficiency as defined above, η_a is the ratio of the beam current to the discharge current and η_e is a measure of the ion acceleration efficiency given by the following equation:

$$\eta_e = \left(\frac{e}{2 m_{Xe} V_d} \right) \left(\frac{T}{I_{beam}} \right)^2$$

Table 3 shows a comparison of the experimental values of these parameters for the SPT-100 as measured by Kim and Bishaev and for the BPT-4000 Hall thruster.[20]

Table 3 - Efficiency Comparison of SPT-100 and BPT-4000 Hall Thrusters

Parameter	SPT-100	BPT-4000
η_u	0.95	0.71
η_a	0.67	0.55
η_e	0.84	1.50
η	**0.54**	**0.59**

These results show that while the propellant utilization efficiency of the BPT-4000 is lower than that of the SPT-100, the voltage losses in the BPT-4000 are significantly lower than in the SPT-100. The comparison illustrates that BPT type thrusters have different operating characteristics than SPT type thrusters.

Of comparable magnitude to the energy deposition in the anode are the radial losses in the plume. Figure 4 shows a characterization of these losses as a function of angle. The plot demonstrates that

although Faraday cup measurements at 1 m show ion current fractions greater than 5% at angles greater than 35°, the total power contained in this current is negligible.[6,8]

Figure 4 - Radial Losses as a Function of Angle from Centerline

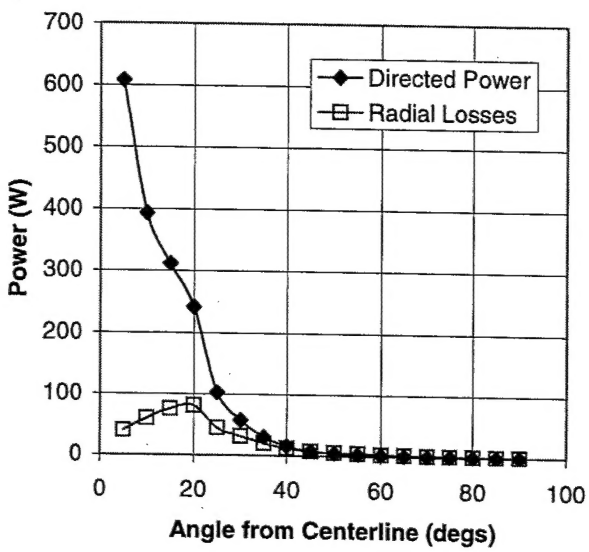

The primary losses are due to ions which have been accelerated through the full accelerating voltage but leave the thruster at angles between 5° and 25°. These results are consistent with LIF measurements made on the SPT-140 by Pollard et al as well as numerous other measurements made by other researchers of radial ion acceleration using Faraday probes, mass spectroscopy and LIF.[6] It has been postulated that these losses are the result of a large fraction of the ion acceleration occurring downstream of the exit plane in a region of convex magnetic field lines.[7] The magnitude of these losses suggests that additional focusing of the ion beam would be another avenue for improving the performance of the BPT-4000. The measurements also suggest that while calculations of the half angle enclosing 90 or 95% of the current may be useful for spacecraft integrators, comparing the ratio of the current at 20 degrees to that at 5 degrees is a much better measure of the ion beam focusing.

The last significant fraction of the losses is due to energy deposition in the insulator rings from electron and ion collisions. The percentage of the heat generated by ion collisions can be estimated using Aerojet's erosion model since the sputter rate is directly proportional to the ion flux times the average ion energy. These calculations show that the ion current flux to the wall is approximately 3 A and the average ion energy is 50 eV for a total power deposition due to ion-wall collisions of 150 W or 5% of the total thruster power. This result again demonstrates that additional performance gains could be achieved if the ion beam could be focused in such a way that radial acceleration of the ions was reduced. Not only would such improvements increase the performance of the device, reductions in the radial component of ion velocity would also increase the lifetime by reducing the insulator wall erosion. The remainder of the power deposited in the insulator rings is the result of electron-wall collisions.

CONCLUSIONS

Detailed calculations of the energy losses in the BPT-4000 Hall thruster have been performed. Comparison of the results to measurements of thruster efficiency and input power show excellent agreement. The calculations shows that energy deposition in the anode and insulator rings and radial kinetic energy of the ions are the dominant loss mechanisms. The dominant loss mechanisms in the BPT-4000 are also shown to differ significantly from those in the SPT-100 supporting the conclusion that BPT type thrusters have some different operating characteristics than other magnetic layer thrusters.

The dominant loss mechanisms result from two key phenomena - radial acceleration of ions outward from the channel centerline and infrequent collisions between electrons and neutrals in the ionization region. Together the losses from these mechanisms account for nearly 33% of the total input power to the thruster. It is likely that both of these phenomena can be influenced by changes in the discharge channel and magnetic field designs. This conclusion is supported by the higher propellant utilization efficiency of SPT type thrusters. Therefore, it is reasonable to conclude that despite the recent maturation of Hall thruster technology, additional performance gains can be achieved and the operating envelope of these devices can be expanded.

REFERENCES

[1] S. Oleson, et al., "Advanced Propulsion for Geostationary Orbit Insertion and North-South Station Keeping," Journal of Spacecraft and Rockets, Vol. 34, No. 1, January 1997.

[2] S. Oleson and R. Myers, "Launch Vehicle and Power Level Impacts on Electric GEO Insertion,"

AIAA-96-2978, AIAA/ASME/SAE/ASEE Joint Propulsion Conference, August, 1996.

[4] J. Fisher, et al., "The Development and Qualification of a 4.5 kW Hall Thruster Propulsion System for GEO Satellite Applications," AIAA/ASME/SAE/ASEE Joint Propulsion Conference Proceedings, July, 2003.

[5] K. de Grys, et al, "Extended Duration Life Testing of 4.5 kW Flightweight Hall Thruster," JANNAF Conference Proceedings, November, 2002.

[6] J. Pollard and E. Beiting. "Ion Energy, Ion Velocity, and Thrust Vector Measurements for the SPT-140 Hall Thruster," 3rd International Conference on Spacecraft Propulsion, Cannes, France, October 2000.

[7] J. Haas and A. Gallimore. "Characterization of the Internal Plasma Structure of a 5 kW Hall Thruster," IEPC-99-078, 21st International Electric Propulsion Conference, Japan, 1999.

[8] J. Pollard, et. al, "Ion Flux, Energy, and Charge-State Measurements for the BPT-4000 Hall Thruster," 37th AIAA/ASME/SAE/ASEE Joint Propulsion Conference Proceedings, July, 2001.

[9] D. King and K. de Grys, "Multi-mode Hall Thruster Development," 2001 AIAA/ASME/SAE/ASEE Joint Propulsion Conference Proceedings, July, 2001.

[10] L. King and A. Gallimore, "Ion Energy Diagnostics in the Plume of an SPT-100 from Thrust Axis to Backflow Region," 34th AIAA/ASME/SAE/ASEE Joint Propulsion Conference Paper AIAA-98-3641, Cleveland, OH, July 1998.

[11] S. Pullins, et al. "Ion Dynamics in Hall Effect and Ion Thrusters: $Xe^+ + Xe$ Symmetric Charge Transfer," 38th Aerospace Sciences Meeting, Reno, NV, January 2000.

[12] I. Katz, et al. "A Hall Effect Thruster Plume Model Including Large-Angle Elastic Scattering," AIAA-2001-3355, 37th AIAA/ASME/SAE/ASEE Joint Propulsion Conference, Salt Lake City, UT, July 2001.

[13] F. Gulczinski and A. Gallimore. "Near-Field Ion Energy and Species Measurements of a 5-kW Hall Thruster," Journal of Propulsion and Power Vol. 17 No. 2, March-April 2001.

[14] D. Manzella. "Stationary Plasma Thruster Plume Emissions," IEPC-93-097, International Electric Propulsion Conference, Seattle, WA, September 1993.

[15] T.R. Sarver-Verhey. "Extended Test of a Xenon Hollow Cathode for a Space Plasma Contactor," IEPC-93-020, International Electric Propulsion Conference, Seattle, WA, September 1993.

[16] A. Salhi. "Theoretical and Experimental Studies of Orificed Hollow Cathode Operation," Ph.D. Thesis, Ohio State University, 1993.

[17] J. Haas and A. Gallimore. "An Investigation of Internal Ion Number Density and Electron Temperature Profiles in a Laboratory-Model Hall Thruster," AIAA-00-3422, 36th AIAA/ASME/SAE/ASEE Joint Propulsion Conference, Huntsville, AL, July 2000.

[18] A.M. Bishaev and V. Kim. "Local Plasma Properties in a Hall-current Accelerator with an Extended Acceleration Zone," Soviet Physics-Technical Physics, Vol. 32 No. 9, 1978.

[19] D. King, et al. "Magnetic Flux Shaping in Ion Accelerators with Closed Electron Drift," United States Patent No. 6,208,080 B1, March, 2001.

[20] J. M. Fife and M. Martinez-Sanchez. "Two-Dimensional Hybrid Particle-In-Cell Modeling of Hall Thrusters," IEPC-95-240, 17th International Electric Propulsion Conference, 1995.